Energy
Ontario

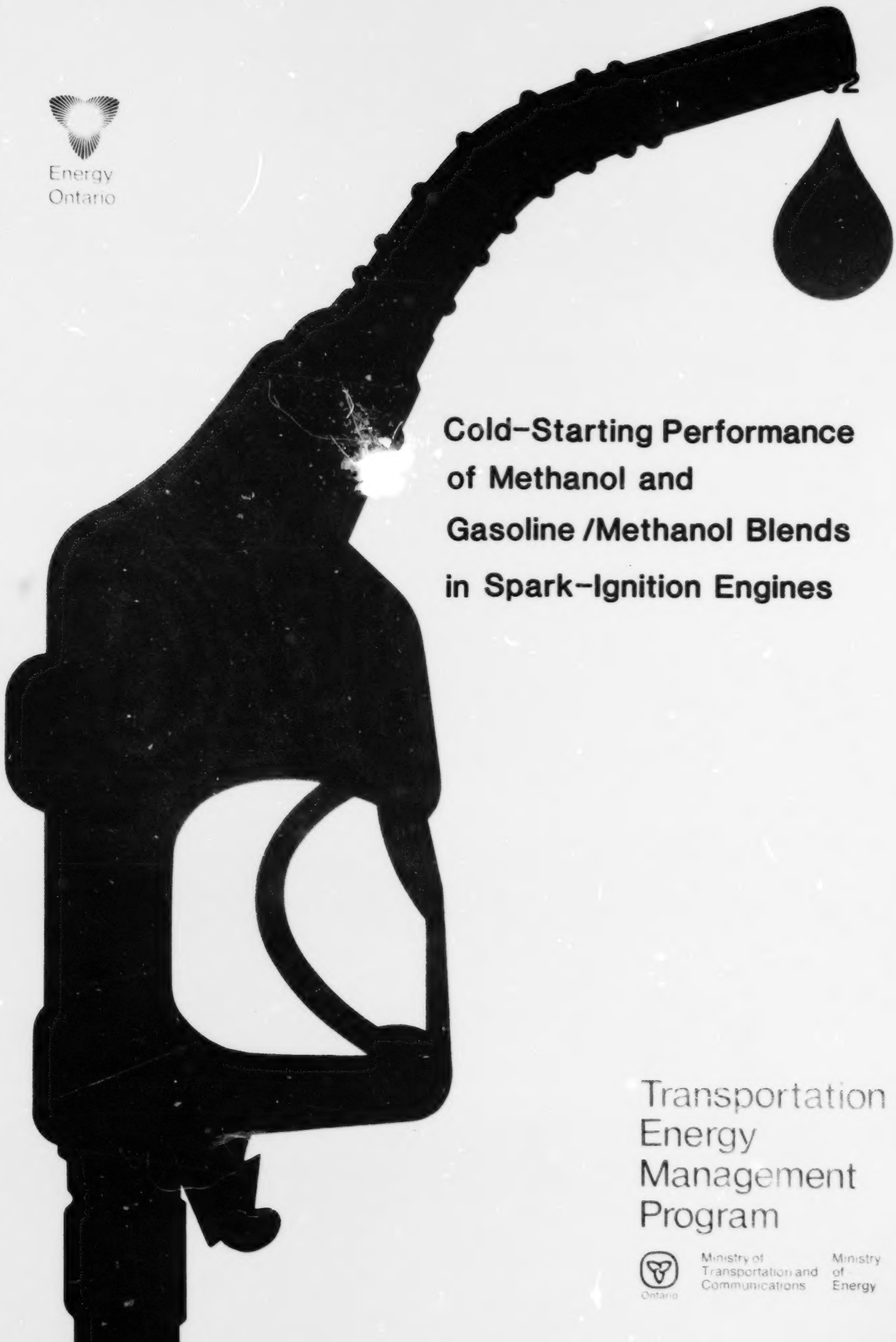

Cold-Starting Performance of Methanol and Gasoline/Methanol Blends in Spark-Ignition Engines

Transportation
Energy
Management
Program

Ontario
Ministry of Transportation and Communications
Ministry of Energy

AF-84-02

Cold-Starting Performance of Methanol and Gasoline/Methanol Blends in Spark-Ignition Engines

M. F. Bardon
Associate Professor

V. K. Rao
Senior Research Engineer

D. P. Gardiner
Technical Officer

Department of Mechanical Engineering
Royal Military College of Canada
Kingston, Ontario

Published by:
The Transportation Energy Management Program

Transportation Technology and Energy Branch
Ontario Ministry of Transportation and Communications
Hon. James W. Snow, Minister
H. F. Gilbert, Deputy Minister

Ontario Ministry of Energy
Hon. Philip Andrewes, Minister
G. R. Thompson, Deputy Minister

Published without prejudice
as to the application of the findings.
Crown copyright reserved; however, this
document may be reproduced for non-commercial
purposes with appropriate attribution.

For additional copies write:
The Editor, Technical Publications
Ministry of Transportation and Communications
1201 Wilson Avenue
Downsview, Ontario
M3M 1J8

November 1983

Technical Report Documentation Page

MTC Report Number AF-84-02	ISBN Number:	Other Document Number:	Date: April 1984

Title: Cold-Starting Performance of Methanol and Gasoline/Methanol Blends in Spark-Ignition Engines

Authors (name, title and/or organisation):
M.F.Bardon, Associate Professor; V.K.Rao, Senior Research Engineer; D.P.Gardiner, Technical Officer; Royal Military College of Canada

Published by:
The Transportation Technology and Energy Branch, MTC
Ontario Ministry of Energy

Client Group:
Transportation Energy Management Program

Participating Agencies:

Abstract:
This report describes a research program conducted in the Mechanical Engineering Department of the Royal Military College of Canada on the cold-starting performance of methanol and several 90% gasoline/10% methanol blends.
Starting trials were conducted using a small spark-ignition engine in a cold test chamber. Test results given show the influence of fuel/air ratio on the minimum temperature at which starting could be obtained using the various fuels.
A preliminary mathematical model was developed which includes the effects of heat loss to the cold cylinder walls and fuel evaporation. The mode assumed continuous shifting vapour/liquid equilibrium throughout the compression process. Predicted results were compared to experimental data. The model proved capable of defining the best cold-starting performance possible for methanol; however, fuel evaporation rate effects change the fuel/air ratio at which this performance actually occurs in the real engine. For the M10 mixtures, evaporation rate effects predominate and must be added to the model if it is to accurately predict the performance of such blends.

Key Words: Cold-Starting Performance, methanol, gasoline/methanol blends, spark ignition engines,

Comments:

Distribution: by request

Copyright Status: Crown copyright

FOREWORD

This project was carried out as part of the Transportation Energy Management Program undertaken by the Ontario Ministry of Transportation and Communications in conjunction with the Ministry of Energy. The program is aimed at reducing Ontario's dependence on conventional liquid petroleum resources in the transportation area and supports a range of projects concerned with the utilization of various alternative fuels.

PROGRAM SUPPORT AND ACKNOWLEDGEMENTS

This program was conducted from March until July 1983 in the laboratories of the Department of Mechanical Engineering, Royal Military College of Canada, Kingston. Major apparatus and facilities were supplied by the Department of National Defence and funding for personnel and additional equipment costs were provided by the Ontario Ministry of Transportation and Communications and the Ontario Ministry of Energy under OJT and CRP Project #33360.

The assistance of the following is gratefully acknowledged:

D. Elliott	MTC -- program definition and monitoring,
G. Caird	RMC -- laboratory assistance during cold-start testing,
W. Davies	RMC -- fuel analysis, and
J. Thibault	RMC -- assistance in report preparation.

ABSTRACT

This report describes a research program conducted in the Mechanical Engineering Department of the Royal Military College of Canada on the cold-starting performance of methanol and several 90% gasoline/10% methanol blends.

Starting trials were conducted using a small spark-ignition engine in a cold test chamber. Test results given show the influence of fuel/air ratio on the minimum temperature at which starting could be obtained using the various fuels.

A preliminary mathematical model was developed which includes the effects of heat loss to the cold cylinder walls and fuel evaporation. The model assumed continuous shifting vapour/liquid equilibrium throughout the compression process. Predicted results were compared to experimental data. The model proved capable of defining the best cold-starting performance possible for methanol; however, fuel evaporation rate effects change the fuel/air ratio at which this performance actually occurs in the real engine. For the M10 mixtures, evaporation rate effects predominate and must be added to the model if it is to accurately predict the performance of such blends.

TABLE OF CONTENTS

	PAGE
FOREWORD	ii
PROGRAM SUPPORT AND ACKNOWLEDGEMENTS	iii
ABSTRACT	iv
NOMENCLATURE	viii
1/ INTRODUCTION	1
2/ SCOPE OF THE PRESENT STUDY	2
3/ FUELS TESTED	3
4/ EXPERIMENTAL PROCEDURE	4
4.1/ Fuel Compatibility	4
4.2/ Apparatus	4
4.3/ Fuel Handling	6
4.4/ Procedure During Cold-Starting Trials	6
4.5/ Temperature Measurements Inside the Cylinder	7
5/ MATHEMATICAL MODEL OF COLD-STARTING	9
5.1/ Basic Assumption Concerning Phase Equilibrium	9
5.2/ Engine Geometry	9
5.3/ Heat Transfer	10
5.3.1/ One Dimensional Assumption	11
5.3.2/ Heat Transfer Rate	11
5.4/ Basic Thermodynamic Properties	12
5.5/ Fuel Volatility	14
5.6/ Phase Distribution	16
5.7/ Finite Difference Equations	17
5.8/ Computer Model	17

PAGE

6/ EXPERIMENTAL RESULTS AND DISCUSSION 19
6.1/ Cold-Starting Trials 19
6.2/ Cylinder Temperature Measurements 21
6.3/ Phase Separation of M10 Blends 22

7/ MODEL PREDICTIONS AND COMPARISON WITH EXPERIMENTAL RESULTS . . 24
7.1/ Predicted Temperature During Compression 24
7.2/ Comparison of Predicted and Experimental Cold-Starting Performance 24

8/ CONCLUSIONS 28

9/ REFERENCES 30

10/ APPENDIX A: Properties of The Fuels Tested. 31

11/ FIGURES 34

LIST OF FIGURES

PAGE

1/ Test Engine. 34
2/ Carburettor Fitted with Positioning Jigs to Provide Precise Choke and Throttle Openings. 34
3/ Cold Chamber Showing Variable Speed Cranking Motor and Refrigeration Unit 35
4/ Cranking Motor Arrangement 35
5/ Schematic of Two-Stage Cascaded Refrigeration Unit and Cold Chamber 36
6/ Comparison of the Cold-Starting Performance of Indolene and OMTC M10 for Identical Carburettor Settings. 37
7/ Comparison of the Cold-Starting Performance of OMTC M10 and High Volatility M10. 38
8/ Comparison of the Cold-Starting Performance of Indolene and High Volatility M10. 39
9/ Comparison of the Cold-Starting Performance of Indolene and M10 of Equal RVP 40
10/ Comparison of the Cold-Starting Performance of Methanol and Indolene 41
11/ Measured Cylinder Temperature During the Compression of Air Alone 42
12/ Measured Cylinder Temperature Bands for Air Alone and Air/Methanol (ϕ = 4) 43
13/ Effect of Cranking Speed on Temperature Inside the Cylinder (Air Alone) 44
14/ Predicted Effect of Fuel Evaporation on Temperature Inside the Cylinder. 45
15/ Comparison of Predicted and Measured Cylinder Temperature (Air Alone). 46
16/ Comparison of Predicted and Measured Cylinder Temperature Methanol/Air Mixture (ϕ = 4) 47
17/ Predicted and Experimental Minimum Starting Temperature for Methanol 48
18/ Predicted and Experimental Minimum Starting Temperatures for Indolene 49
19/ Predicted Extent of Vaporization of Indolene and Two M10 Mixtures 50

NOMENCLATURE

A	= instantaneous cylinder surface area or a constant in Equation 12
a	= empirical constant in Equation 2
B	= constant in Equation 12
b	= empirical constant in Equation 2
C	= constant in Equation 12
C_f	= convective heat transfer coefficient, J/m^2Ks
C_p	= constant pressure specific heat kJ/kgK
C_0, C_1, C_2, C_3	= constants in Equation 15
D	= cylinder bore
f	= fuel/air ratio by mass
f_1 and f_2	= functions of VF in Equation 13 and 15
h	= specific enthalpy kJ/kg
k	= thermal conductivity = J/mKs
K	= degrees Kelvin
L	= connecting rod length
M	= molecular weight
M10	= a blend of 90% gasoline and 10% methanol
MTC	= Ontario Ministry of Transportation and Communications
OMTC M10	= M10 fuel supplied by MTC
P	= pressure
P_r	= Prandtl Number = $C_p \mu/k$
$\dot{Q}$	= instantaneous heat loss rate, kW
$\bar{R}$	= universal gas constant = 8.314 J/mol·k
r	= crank throw radius
RVP	= Reid Vapour Pressure [12]
S	= total entropy, kJ/K
s	= specific entropy kJ/kgK
T	= instantaneous bulk mean fluid temperature, degrees Kelvin
t	= time
U	= total internal energy, kJ
u	= specific internal energy, kJ/kg
V	= total volume

v = specific volume m^3/kg

VF = vapour fraction = mass fraction of fuel in the vapour phase

x = piston displacement from Top Dead Centre

Greek

ϕ = fuel/air equivalence ratio = f/f_{st}

θ = crank angle from Top Dead Centre

μ = absolute viscosity, Ns/m^2

Subscripts

o = value at reference conditions

fg = change in value during evaporation

sat = saturation value

st = stoichiometric value

vap = value for the vapour

1/ INTRODUCTION

Methanol or methanol/gasoline blends are among the most attractive alternatives to replace conventional gasoline in spark-ignition engines. Since they can be transported and stored as liquids without pressurization, vehicle and service station hardware need not undergo major modifications to permit their use. In addition to the general compatibility of methanol with existing technology, its production from coal or renewable biomass is both technically advanced and economically attractive compared to other alternative fuels.

Although in most respects, methanol or methanol/gasoline blends are excellent fuels, differences in volatility characteristics such as vapour pressure, evaporation rate and latent heat result in driveability problems in the Ontario climate. In particular, cold-starting and performance during warm-up both deteriorate markedly with these substitute fuels. In the case of gasoline/methanol mixtures, the extent of cold-starting and running problems is at present not completely clear; however, pure methanol causes severe starting difficulties at ambient temperatures which are very mild by Canadian standards -- below about 10°C. Consequently, during a typical winter in this country, methanol-fuelled engines cannot presently be started without dual fuelling, fuel volatility improving additives or special starting hardware. None of these solutions is yet adequate.

Although vehicle and fleet tests are a necessary part of any development program involving alternative fuels, such tests suffer as a diagnostic technique from the large number of uncontrollable variables. These make it very difficult to determine the underlying causes of observed behaviour. As a result, there is a need for more carefully controlled laboratory studies and theoretical analysis in order to elucidate and ultimately overcome the fundamental causes of difficulties. Otherwise, solutions are haphazard, very costly to develop and far from optimum.

The object of this preliminary study is to develop some specific cold-starting performance data under carefully contolled laboratory conditions and to begin work on the mathematical modelling necessary to properly interpret the results. Ultimately, both aspects would contribute to the improved understanding necessary to make methanol fuel technology feasible in Ontario.

2/ SCOPE OF THE PRESENT STUDY

The principal aims of the present study are:

1/ to obtain actual experimental data on the cold-starting performance of a specific commercially prepared 90% gasoline/10% methanol blend supplied by the MTC when used in an unmodified engine as a simple replacement for gasoline;

2/ to develop a preliminary mathematical model of spark-ignition engine cold-starting which would be based on the assumption of continuous shifting vapour/liquid equilibrium during compression (i.e., not including any effects due to fuel evaporation rate);

3/ to conduct experimental cold-starting tests on fuels chosen so that the results could be used to evaluate the mathematical model;

4/ to use the theoretical and experimental results to help define further studies needed to develop automotive alcohol fuel technology appropriate for Ontario.

3/ FUELS TESTED

In addition to the fuel supplied by the MTC, several other test fuels were used during the trials. M10 mixtures to be used commercially must be blended to meet the same overall specifications as straight gasoline. This requires that the gasoline components be modified so as to control several fuel properties. These changes complicate the experimental evaluation of performance because some of the observed differences between such an M10 and ordinary gasoline are due to the changed hydrocarbon portion rather than solely to the effects of the alcohol.

In order to clarify the relative influence of the changes in the gasoline base stock, tests were also run on special blends prepared using Indolene as the base stock. Two combinations were produced:

1/ a straight 90% Indolene/10% methanol mix which, as a result, had a substantially higher Reid Vapour Pressure than the original Indolene and

2/ a mixture of 10% methanol and 90% of an Indolene which had been previously heated mildly to reduce its vapour pressure, such that the resulting M10 would have a Reid Vapour Pressure identical to that of the original Indolene. Appendix A gives property data for all the test fuels.

Tests were also run on pure methanol, as well as the M10 mixtures, so as to have experimental data to compare with the simplest version of the mathematical model -- that of single component fuel.

4/ EXPERIMENTAL PROCEDURE

4.1/ Fuel Compatibility

The major concern of this preliminary work is merely to establish what modifications, if any, were required before the candidate alcohol fuels could be used in the test apparatus previously developed for conventional gasoline. No attempt was made to evaluate long-term corrosion problems.

Although some minor swelling of gaskets was observed, this did not disable the apparatus in any way. The only significant effect of alcohol on the original engine components was the swelling and jamming of the carburettor float, which was made of an unknown synthetic material. By coating the stock float in the so-called "hot fuel proof dope" sold for model airplane construction, the swelling was controlled long enough to conduct the cold-starting tests without difficulty. The float did, however, eventually swell and jam, so the OMTC M10 would obviously not be used as a simple substitute without modifications to at least some existing carburettors. It is interesting to note that swelling, though present, was much less pronounced with the two M10 blends produced especially for this test progr-m. With these two fuels, the carburettor float did not swell badly enough to require coating. Only pure methanol and the OMTC M10 could not be used in the original carburettor, and in fact, swelling was more rapid when the float was immersed in the OMTC M10 than in the pure methanol.

4.2/ Apparatus

The tests were performed in a two-cylinder Military Standard Engine Model 2A016III (Figure 1). This is a four-stroke overhead valve air-cooled engine of 262 cm^3 (16 in^3) displacement manufactured by Chrysler Outboard Corporation. The nominal compression ratio is 6:1 and rated power is 2.24 kW (3 hp) at 3600 RPM. The actual geometric compression ratio was measured by the liquid displacement technique and found to be 5.84:1.

The stock carburettor has an adjustable main jet. This made possible the considerable change in jet size needed to permit appropriate fuel/air ratios for both methanol and gasoline. The only carburettor modifica-

tions for the gasoline tests were the attachment of positioning jigs to give repeatable throttle and choke settings. Figure 2 shows the carburettor fitted with the jigs.

Several other carburettor modifications were necessary for the pure methanol tests. As mentioned already, the stock synthetic float material swelled badly and jammed when soaked in the alcohol. Therefore, an external float bowl with brass float was used instead, vented to the carburettor inlet and positioned so that the fluid was at the appropriate level with respect to the jets. To permit the larger volumetric fuel flow rates required for methanol, the mixture adjustment needle was retracted completely from the main jet orifice and the fuel inlet passage to the carburettor was enlarged.

For the tests on gasoline/methanol blends, the standard carburettor was used after the float was coated, as described earlier, to prevent excessive swelling.

A variable speed electric motor supplied by a variable transformer was used to crank the engine during the trials. An electric tachometer was permanently mounted. Cranking speed normally kept within 2% of the prescribed value on any given test. Figures 3 and 4 show the test chamber and cranking motor.

The engine was mounted in an insulated cold test chamber cooled by a specially constructed two-stage vapour-compression refrigeration unit capable of providing chamber temperatures as low as -65°C. Figure 5 shows a schematic of the refrigeration unit.

Fuel/air ratios were determined by calibrating the carburettor. At the low cranking speeds involved in engine starting, the air flow through the induction system undergoes substantial pulsing as valves open and close. This produces a similar pulsing in the fuel circuit although as a lesser amplitude. There are also some fluctuations due to the operation of the carburettor float valve. In order to determine the mean fuel/air ratio at any given carburettor setting and RPM, the total fuel flow was measured over a time interval sufficiently long to keep the error due to pulses less than the precision with which the flow was measured. This

was accomplished using a calibrated burette and a stop-watch. The air-flow over the same interval was found by using a large volume airbox which damped out the oscillations, permitting the steady mean flow to be measured with a standard orifice [1] and a water manometer.

4.3/ Fuel Handling

In the case of any multicomponent fuel, evaporation changes the composition and volatility. As a result, it is essential, when dealing with the highly volatile fuels concerned here, to minimize evaporation during handling and storage.

General handling procedures during this program included storing the fuels in sealed containers in which the liquid level was kept at greater than 70% of full capacity and effecting transfers quickly and at low temperature when possible.

In addition to the potential loss of volatility in storage and when refilling the engine fuel tank, there are also two sources of loss in the engine itself. Both the carburettor float bowl and the fuel tank are ordinarily vented. For this test program, the fuel tank was specially fitted with a check valve so that, whereas air could enter as fuel level dropped during a starting test, no fuel vapour could escape. The tank was also kept topped up using a container of fuel kept in the test chamber so that it would be cold during the transfer process. Significant evaporation from the carburettor float bowl vent was avoided by shutting the stop-cock from the fuel tank and emptying the float bowl after each test. The valve was then only reopened immediately prior to closing the chamber and beginning the cold-soak period.

4.4/ Procedure During Cold-Starting Trials

Prior to each test, spark plugs were removed, dried if wet from the previous test, cleaned if required and electrode gap checked. With the plugs removed, the cylinders and entire induction system were purged of fuel by forcing compressed air through the plug holes.

After this initial preparation, the fuel was supplied to the carburettor, then the engine was cold-soaked long enough to ensure a uniform test temperature throughout, which normally required from one to two hours. This soak time was determined to be adequate by measuring the temperature at various locations inside the engine, including the combustion chamber, and by repeating tests using longer soak times to verify the results. These cold-soak times are considerably shorter than those required for typical automotive engines because the engine is small, air-cooled and has an aluminum cylinder block and heads.

The test sequence was standardized so as to get consistent comparative readings. For all the results reported here, the standard cranking speed was 600 RPM and the throttle was held 20° open. The choke was used to produce the desired fuel/air ratio. Based on considerable preliminary work, the best procedure found was to use three 10 sec bursts of cranking with a 10 sec pause between bursts. The engine was considered to have successfully started if it achieved self-sustained running after the starter bendix gear disengaged. It was observed that mixtures just slightly too lean would result in erratic firing sufficient to disengage the starter without leading to sustained running.

4.5/ Temperature Measurements Inside the Cylinder

Temperature measurements were made inside the cylinder during cold cranking by means of a very fast response 1 μm diameter platinum resistance thermometer (constant current hot-wire anemometer).

The probe was held in a fixed position protruding into the centre of the combustion chamber in a specially built mount fitted into the normal spark plug hole.

The advantage of this technique over the use of a pressure transducer is that temperature is measured directly rather than being calculated indirectly from pressure using rather uncertain volume and trapped gas mass estimates. It has the further advantage of directly indicating temperature fluctuations if any exist. In the case of a pressure transducer, output fluctuations could be due to either pressure or temperature varia-

tions or both. The constant current hot wire technique gives unambiguous temperature data.

For all tests reported here, a DISA 55P31 probe was used in conjunction with a DISA 55M20 Temperature Bridge and a Honeywell Visicorder Model 1858 for data recording.

5/ MATHEMATICAL MODEL OF COLD-STARTING

5.1/ Basic Assumption Concerning Phase Equilibrium

As described earlier, the basis of the mathematical model at this stage of the work was to assume that the fuel liquid and vapour remain continuously in phase equilibrium as the compression process proceeds. As long as any liquid fuel remains, the partial pressure of the fuel will then be exactly equal to the saturation pressure for the conditions existing at any point in the process.

In order that this assumption be valid, evaporation rate must be very fast compared to the rate of change of the other variables such as temperature and pressure. This requires not only rapid diffusion of fuel vapour away from the evaporation droplets, but also very fast heat transfer between liquid droplets and the surrounding gaseous medium so that droplet temperature remains at all times equal to gas temperature. In reality, both heat transfer and diffusion occur at finite rates; consequently, droplet temperature lags behind gas temperature and fuel partial pressure is less than the saturation value.

The intention in making this assumption was to determine to what extent the fundamental equilibrium volatility limits cold-starting performance and to see what useful conclusions might be drawn about the relative importance of evaporation rate by comparing real data with equilibrium predictions. It was expected that this assumption would be relaxed in later extensions of the mathematical model.

5.2/ Engine Geometry

Piston motion can be expressed as a function of crankshaft angle using an equation of the following form [2]:

$$x = r(1 - \cos\theta + \frac{r}{2L}\sin^2\theta) \qquad (1)$$

where: x = piston displacement from Top Dead Centre
r = crank throw radius (= stroke/2)

L = connecting rod length

Θ = crank angle from Top Dead Centre (i.e.: during a compression stroke, Θ varies from 180° at BDC to 360° at TDC)

Coupled with cylinder bore, this equation is also used to calculate instantaneous volume swept by the piston. Adding the known volume at Top Dead Centre gives total instantaneous cylinder volume. Total instantaneous cylinder surface area is found in a similar way, using Equation 1, bore, and the surface area of the piston face and cylinder head.

Some additional assumptions were also used to determine the mass of gas trapped in the cylinder. Leakage past the rings was presumed negligible and the intake valve closure was taken to occur at Bottom Dead Centre. This latter is not strictly true; however, because heat transfer calculations were based on previous experimental data obtained with this same engine, the error is slight for the results presented in this report. The model itself can begin the compression start point at any value of Θ so as to accommodate whatever value timing a given engine might have.

Engine cranking speed during cold-starting is low. Consequently, the model does not take into account any charging effect due to air velocity in the induction system. The mass of fluid trapped in the cylinder on intake valve closure is found from cylinder geometry at that point along with intake manifold discharge temperature and pressure.

If cranking were continuous during a cold-starting experiment, then the intake manifold discharge temperature would be lower than ambient due to the cooling effect of fuel evaporation. The mathematical model can predict this temperature drop. However, the starting procedure found to be most effective includes pauses between bursts of cranking. This allows the cooler-than-ambient charge to warm back up and also provides time for fuel evaporation. Consequently, in the theoretical predictions reported here, the start point of the compression process was assumed to be equilibrium at ambient temperature.

5.3/ Heat Transfer

5.3.1/ One Dimensional Assumption

This model uses bulk fluid properties; that is, temperature and pressure gradients are assumed negligibly small. This approach has been used extensively in engine cycle models and, though very restrictive for combustion modelling, is, in fact, quite well-substantiated experimentally for the compression process of interest for a cold-starting analysis. Another simplification is also possible for this special case. Because of the vast mass of metal in the block, its high thermal conductivity and the low thermal capacity of the air, the cylinder wall temperature rises a very small amount during cold cranking. It is therefore assumed that the walls of the cylinder remain at ambient temperature throughout the compression and attempted ignition process.

5.3.2/ Heat Transfer Rate

The film coefficient for heat transfer between the air and the cylinder wall was calculated using the relation developed by Annand [3], namely

$$C_f = a\, C_p \mu\, Re^b / D\, Pr \qquad (2)$$

where: C_f = convective heat transfer coefficient, J/m^2Ks
a and b = empirical constants for the particular engine concerned
C_p = constant pressure specific heat, kJ/kgK
μ = absolute viscosity, Ns/m^2
D = cylinder bore
Pr = Prandtl number
Re = Reynolds number based on mean piston speed and instantaneous fluid properties

In this equation, Annand's term accounting for radiation has been omitted because it is negligible in the case of cold-starting due to the low temperatures. In order to evaluate the film coefficient at any given conditions, mixture properties were required. The Prandtl number was taken to be 0.70 and the following equation was used to evaluate absolute viscosity:

$$\mu = \frac{2.27 \times 10^{-8}(T)^{1.5}}{T + 198.6} \qquad (3)$$

Using the film coefficient C_f found from Annand's Equation, the instantaneous heat transfer rate between the working fluid and the cylinder walls can be calculated using the basic convective heat transfer equation:

$$\dot{Q} = C_f A(T - T_{walls}) \qquad (4)$$

where: $\dot{Q}$ = instantaneous rate of heat loss to the cold cylinder walls
A = instantaneous cylinder surface area
T = instantaneous fluid temperature (i.e., bulk mean temperature by virtue of the basic assumptions)
T_{walls} = temperature of the piston and cylinder surfaces to which heat is lost (= ambient temperature as stated above)

5.4/ Basic Thermodynamic Properties

The ideal gas law was used as the equation of state for the various gases and vapours concerned, generally in the following form:

$$PV = \frac{\bar{R}}{M} T \qquad (5)$$

where: P = partial pressure of the gas concerned
V = total volume
m = mass of the gas
$\bar{R}$ = universal gas constant
M = molecular weight of the gas
T = absolute temperature

Over the entire range of temperatures involved in these test, specific heats of the gases concerned are essentially constant. Values at room temperature were therefore used throughout.

The mean specific heat of the gaseous portion of the mixture was calculated using a weighted average based on the instantaneous proportions of

air and fuel vapour. Other gas properties such as mean molecular weight were similarly found. The assumption of constant specific heat for the gases simplifies the determination of other properties as well. Enthalpy h is determined by

$$h = h_0 + C_p(T - T_0) \tag{6}$$

where: h = enthalpy per unit mass
C_p = specific heat at constant pressure
T_0 = reference temperature
h_0 = arbitrary value of h at the reference temperature

Internal energy u is calculated from enthalpy using the basic definition

$$u = h - Pv \tag{7}$$

where P = partial pressure of the component
v = specific volume

Entropy for a gas is found from the following expression

$$s = s_0 + C_p \ln (T/T_0) - \frac{\bar{R}}{M} \ln (P/P_0) \tag{8}$$

where: s = specific entropy
s_0 = arbitrary value of s at the reference conditions
P_0 = reference pressure

For liquids, Equations 6 and 7 apply equally and the corresponding entropy equation is Equation 8 without the last term.

On evaporation, the enthalpy increases by a value equal to the latent heat (enthalpy of evaporation) h_{fg}. Vapours thus have both a sensible enthalpy component determined by Equation 6 and a latent component. The total enthalpy of the fuel vapour is therefore given by

$$h = h_0 + h_{fg}^{\ell} + C_p(T - T_0) \tag{9}$$

where: h_{fg}^0 = value of h_{fg} at T_0

h_0 = arbitrary reference value for the liquid fuel at T_0

Similarly, the entropy of fuel vapour is computed from

$$s = s_0 + s_{fg}^0 + C_p \ln (T/T_0) - \frac{\bar{R}}{M} \ln (P/P_0) \qquad (10)$$

where: s_{fg}^0 = entropy of evaporation = h_{fg}^0/T_0

s_0 = arbitrary value for the liquid at T_0 reference

For the entire mixture, the total value of any property is then simply the weighted sum of the values for the various components in a form such as the following for enthalpy.

$$H = m_{air} h_{air} + m_{liq} h_{liq} + m_{vap} h_{vap} \qquad (11)$$

where: H = total mixture enthalpy
m = mass of the given component

5.5/ Fuel Volatility

For a pure single-component fuel such as methanol, vapour pressure is a function of temperature only and can be calculated using the Antoine Equation [4]

$$\text{Log}_{10} P_{sat} = A - B/(C + T) \qquad (12)$$

where: P_{sat} = fuel saturation pressure
A,B,C = constants for the particular substance concerned
T = temperature

For a multicomponent fuel such as gasoline or gasoline/methanol blends, vapour pressure behaviour is much more complex because it is not solely a function of temperature as in the case of a pure fuel, but depends also

on the degree of vaporization. At present, there exists no simple means of calculating the vapour pressure of real fuel mixtures.

The technique used to calculate vapour pressure of the gasoline and M10 mixtures is one developed at RMC as part of another program [5]. The method is based, in part, on the Bridgeman Equilibrium Air Distillation method [6]. Bridgeman's technique uses the ASTM Distillation [7] data for the fuel to produce graphs relating temperature, percentage of fuel evaporated and air/fuel ratio. The difficulty is that the construction and use of the graphs is very tedious and time consuming and the results are of limited application because of the form of the variables used. It is also not amenable to computer calculations.

The method developed uses the ASTM distillation data and the specific gravity as the defining characteristics for volatility. By various manipulations described in Reference 5, an equation is derived of the following form:

$$P_{sat} = f_1 \exp(- f_2/T) \qquad (13)$$

where: P_{sat} = fuel saturation pressure
f_1 = function of vapour fraction VF
f_2 = function of vapour fraction VF
T = absolute temperature
VF = vapour fraction = mass fraction of fuel in the form of vapour at equilibrium

Using computer programs developed during the other study [5], the values of the functions f_1 and f_2 were determined for each fuel to be modelled for values of vapour fraction ranging from zero to one (i.e.: no evaporation to complete evaporation). Using a least squares approximation by cubic spline, curves were fitted to f_1 and f_2 so that saturation pressure could be determined explicitly as a function of T and VF. Mean molecular weight of the vapour and enthalpy of evaporation are also both functions of VF. As part of the calculations, curves were also fitted to their calculated values.

Appendix A gives the actual equations fitted for the various test fuels modelled.

5.6/ Phase Distribution

In order to evaluate total entropy, internal energy and other properties, it is necessary first to determine the proportions of liquid fuel and fuel vapour for the given instantaneous temperature and cylinder volume.

For a single component fuel this procedure is straightforward because temperature uniquely determines fuel saturation pressure in accordance with Equation 12. Since liquid volume is negligibly small, the cylinder volume is essentially equal to the volume of fuel vapour existing at its partial pressure P_{sat}. The ideal gas law then allows the mass of fuel vapour to be determined:

$$m_{vap} = P_{sat}VM/\bar{R}T \qquad (14)$$

where: m_{vap} = mass of fuel vapour
V = cylinder volume
M = fuel molecular weight
$\bar{R}$ = universal gas constant
T = absolute temperature

This equation only holds, of course, provided there is still some liquid fuel present in the cylinder. Once the last drop of fuel evaporates, the fuel partial pressure becomes less than the saturation pressure corresponding to the temperature concerned. in that case, the mass of fuel vapour equals the total mass of fuel originally present, rather than that given by Equation 14 above.

For multicomponent fuels, the same basic procedure applies except that volatility is a function of both temperature and extent of vaporization. Consequently, iteration is required to find m_{vap} based on both T and cylinder volume V. The procedure is to assume a vapour fraction VF, calculate P_{sat}, molecular weight, etc., then use Equation 14 to calculate the mass of vapour which would be present in the cylinder at that value of P_{sat}. If this calculated vapour fraction is not the same as that

originally assumed, then a new value is picked and the procedure is repeated until agreement is reached.

5.7/ Finite Difference Equations

The finite difference forms of the equations were developed from first principles as follows. For some small crankshaft rotation $\Delta\Theta$ before which gas temperature is equal to T_1 and pressure P_1, the piston displacement Δx is calculated from Equation 1. The requirement is to determine the conditions at the end of this incremental compression. During this process, cylinder volume decreases, which tends to increase pressure and temperature. On the other hand, the simultaneous heat transfer (which occurs at rates dependent on the instantaneous temperature difference in accordance with Equation 4) tends to decrease temperature and pressure.

The finite difference solution is developed by breaking the simultaneous heat transfer and compression into two separate stages: an adiabatic and reversible (i.e., isentropic) compression followed by a constant volume heat transfer. The overall compression, therefore, becomes a sawtooth-style series of small isentropic compressions each followed by an isochoric heat loss based on the mean temperature during the previous isentropic step. As the increment $\Delta\Theta$ approaches 0, the finite difference solution approaches the exact case.

5.8/ Computer Model

Using the various individual calculation techniques, each incremental step of the two-phase compression process is found as follows.

1/ Total entropy S_1 is evaluated at the start conditions of the increment using Equations 8, 10, etc.
2/ The new volume V_2 is determined using Equation 1.
3/ An iterative procedure is then used to determine state 2S (i.e., that state which would exist after an isentropic compression to the new volume V_2 such that $S_2 = S_1$). Iteration is required because temperature is not explicitly known in terms of entropy. A trial T_{2S} is chosen, which, in conjunction with V_2, determines all other properties

including S_2. If this S_2 is not equal to S_1 within the specified accuracy, a new trial T_{2S} is chosen and the procedure continues until $S_2 = S_1$.

4/ The average temperature during the hypothetical isentropic increment is then used to determine fluid properties for the determination of the convective heat transfer coefficient in Equation 2. Equation 4 then gives the mean heat loss rate, again using average temperature during the isentropic step.

5/ The total heat lost, Q, during the time increment Δt corresponding to $\Delta\theta$ is then merely the product of mean heat loss rate and Δt.

6/ For a constant volume heat loss, the First Law of Thermodynamics then becomes $U_2 = U_{2S} - Q$. An iterative procedure similar to that described in step 3 above is then used to find T_2 such that this equation is satisfied. These conditions then define the start conditions for the next increment.

Following this procedure, the conditions throughout the compression process are determined up to and including those at Top Dead Centre. Since the spark is assumed to occur at TDC, the fuel vapour/air ratio must lie within the flammable limits for ignition to occur. Representative values of lean misfire limit were used to evaluate whether or not combustion could theoretically occur.

6/ EXPERIMENTAL RESULTS AND DISCUSSION

6.1/ Cold-Starting Trials

Figure 6 shows a comparison of the cold-starting results obtained with the M10 blend supplied by the Ministry (denoted as OMTC M10) compared to the Indolene used as a standardized gasoline.

In all results presented, mixture strength is defined by means of the fuel/air equivalence ratio ϕ defined as

$$\phi \equiv f/f_{st}$$

where: f = actual fuel/air ratio

f_{st} = stoichiometric fuel/air ratio

Each point on the graph was obtained by conducting numerous starting tests over a range of temperatures using the same fuel/air ratio. Above the point shown, the engine was successfully started whereas starting was unsuccessful below that temperature. The results were found to be repeatable to within about 1°C. The abscissa is the equivalence ratio delivered by the carburettor when Indolene was used. Identical settings produced the OMTC M10 results given on the graph.

This figure shows that over most of the range of fuel/air ratios possible with this carburettor, the OMTC M10 blend gives slightly better starting performance than Indolene (i.e., can be started at slightly lower temperatures for a given choke position). At the two extremes, however, the Indolene starts at temperatures about 5°C colder than found with M10. This is not a serious problem for the low equivalence ratio since it merely means that the choke must be closed slightly more to start the M10 at cool temperatures. At the other extreme however, it means that the coldest temperature at which starting is possible is some 5°C higher for M10 than for Indolene (-39°C versus -44°C). Since the OMTC M10 has a higher Reid Vapour Pressure, this latter result is in opposition to normal gasoline comparisons. Increasing the RVP normally improves the cold-starting performance of a given gasoline. Of course, -39°C still seems quite satisfactory, but it must be remembered that conditions during the

tests conducted here were ideal in most respects. Normal automobile performance would be expected to be poorer because of mechanical deficiencies such as imperfect ignition components, spark gap, cranking speed, etc.

In fact, much of the requirement for increased gasoline volatility in winter is due to the need to compensate for the lack of ideal starting conditions, rather than to an inherent limitation of the summer fuel. The Indolene RVP puts it into the range of summer gasoline in Canada. Winter gasoline would have an RVP up to as much as 103 kPa. The results at very cold temperatures on Figure 6 may be due to phase separation, which was observed to occur with the OMTC M10. This is discussed later in the report.

Figure 7 compares the OMTC M10 with the high volatility M10 fuel produced for these tests by blending 90% Indolene and 10% methanol without suppressing in any way the higher resulting RVP. Results for both fuels are plotted against the equivalence ratio produced by the carburettor when Indolene is used at the same settings. In spite of the higher RVP, the simple M10 blend gives poorer starting performance over virtually the entire range of choke settings. That shows that, although RVP has traditionally been a good indicator of cold-starting performance for gasolines, it is not useful when alcohol blends are involved.

Figures 8 and 9 give comparisons of the two M10 blends (made up using Indolene base stock) with the original Indolene. Figure 8 shows that, even though the RVP is substantially higher for the uncorrected M10 blend, its starting performance shows a deterioration from that of Indolene. It can be seen in Figure 9 that the M10 which had its Indolene component adjusted to keep the blend RVP equal to that of the original Indolene fares even worse, especially at the colder temperatures. This graph does not contain a point for M10 at an equivalence ratio around stoichiometric because the test chamber has no provision for heating, which would be required in order to attain temperatures above that of the laboratory.

Figure 10 shows the results for pure methanol compared to Indolene. These results are discussed in more detail in the next section; however,

two points are noteworthy. The first is that the methanol could not be started at all below about 0°C. The second is that enriching the mixture lowers the starting temperature only a small amount and, beyond a certain point, causes deterioration rather than improvement.

6.2/ Cylinder Temperature Measurements

Figure 11 is a tracing of the temperature measured using the 1 μm diameter platinum resistance thermometer when there was only air in the cylinder. The irregularities about the mean are interpreted as the result of turbulence and non-uniform temperature. Eddies transport fluid of various temperatures past the wire; the size of these fluctuations therefore gives an indication of the extent to which the temperature varies from place to place within the cylinder.

It was uncertain when these tests were begun, whether the very fragile platinum wire would be quickly broken by the impact of the droplets and therefore provide no information concerning the effect of fuel evaporation on cylinder temperature. Eventually, the wire did indeed break but not before sufficient data was obtained for methanol under both stoichiometric and rich conditions.

Figure 12 shows a comparison of the temperatures with air alone compared to a methanol/air mixture. Multiple tracings of temperature profiles were used to obtain the bands shown. Each band gives the range of cylinder temperatures measured during different comparison strokes. A significant lowering of cylinder temperature is evident for the methanol/air mixture. This indicates that evaporation has a significant effect on cylinder temperature.

Although temperatures vary fairly substantially from one compression stroke to the next, there was no progressive increase in temperature observed over the number of cycles using for cold-starting tests. This validates the model assumption of a constant temperature cylinder block.

6.3/ Phase Separation of M10 Blends

It is well known that water addition to gasoline/methanol blends can cause the blend to separate into two distinct liquid phases. Even quite small quantities of water can provoke this separation and unfortunately, the blends tend to be hygroscopic. As a result, even exposure to humid air will, given sufficient time, result in separation. Decreasing temperature results in phase separation with smaller water concentrations.

Great care was taken during handling to keep fuel containers sealed and avoid exposure to the air. Lacking appropriate facilities, no attempt was made to measure the water content of the test fuels; however the methanol used to prepare the M10 blends was certified by the supplier to have less than 0.5% water.

The engine was fitted with a transparent tube connecting the fuel pump and carburettor float bowl. This allowed visual observation of the fuel condition immediately after a test run. Phase separation was observed to occur in two stages. The first was a cloudiness in the normally transparent flow and the second, the appearance of distinct globules of a second liquid phase. Because of the physical arrangement of the engine components and the nature of the test procedure, both phases were fed to the cylinder. The separation which obviously occurred would be expected to change the vapour pressure and hence cold-starting performance, but there was not the problem of induction of only one of the two liquid phases, as might happen in an automobile engine.

The deterioration of cold-starting performance at low temperatures noted in the previous chapter was likely due, at least in part, to the changes wrought by phase separation.

To clarify the range of temperatures over which separation was occurring during the starting trials, transparent containers of the various M10 fuels were cooled in the cold chamber using a thermocouple to measure liquid temperature.

The OMTC M10 exhibited clouding at -15°C and was clearly separated into two phases by -20°C. Since it was initially suspected that the original

sample provided might have been contaminated, a second sample was obtained. However, it produced identical results, suggesting that, if water contamination was responsible, it was occurring previous to delivery to RMC.

The two M10 blends produced for the program by combining Indolene and methanol separated at -13 to -15°C in the case of the high volatility version and at -12 to -13°C for the blend having the same RVP as the Indolene.

7/ MODEL PREDICTIONS AND COMPARISON WITH EXPERIMENTAL RESULTS

7.1/ Predicted Temperature During Compression

Figure 13 shows the effect of cranking speed on temperature within the cylinder when air alone is compressed. As cranking speed increases, heat losses decrease and temperatures throughout the compression are higher. The two extremes -- isentropic compression as RPM $\rightarrow \infty$ and isothermal compression as RPM $\rightarrow 0$ -- are indeed approached at low and high cranking speeds. However, because of the form of Annand's Equation (Equation 2) neither extreme is attainable at reasonable engine speeds because heat transfer is directly proportional to a fractional power of RPM. The area lying between the curves for 10 and 500 RPM likely represents the approximate range for typical cold-starting conditions. Even within this band however, there is obviously considerable variation in heat loss possible by changing cranking speed. This is expected to be important for determining optimum cranking speeds for cold-starting.

Figure 14 shows the predicted cylinder temperatures for air alone, stoichiometric air/methanol and air/Indolene mixtures. The effect of fuel evaporation is a decrease in mixture temperature compared to the case of air alone. As expected, this decrease would be much greater for methanol because of the combined effect of higher enthalpy of evaporation and higher fuel/air ratio at a given stoichiometry.

Figures 15 and 16 show a comparison of predicted and measured temperatures. For air alone the agreement between predicted and measured temperature is quite reasonable. The fluctuations due to non-uniform temperature evidently do not invalidate the use of a bulk mean temperature.

In the case of methanol, however, the measured extent of temperature reduction is considerably smaller than that predicted by the model. This confirms that evaporation lags well behind equilibrium conditions during the compression stroke for these conditions.

7.2/ Comparison of Predicted and Experimental Cold-Starting Performance

Figure 17 shows the measured minimum starting temperatures for pure methanol as well as those predicted by the model for two cases: constant and actual manifold pressure. In the real case, as the choke is closed, the absolute pressure in the intake manifold decreases. This reduces the mass of the change trapped in the cylinder and also decreases the charge density, thereby providing a greater volume into which the fuel evaporates. Reduced charge mass has an adverse effect on starting by reducing the temperature achieved after compression. On the other hand, reduced density improves starting by improving evaporation. The curve on Figure 17 labelled "Actual Manifold Pressure" gives the results calculated by the model when it includes the effect of reduced manifold pressure caused by closing the choke in order to increase ϕ. For comparison, the case of constant manifold pressure (equal to ambient pressure) is also shown, labelled "Constant Manifold Pressure".

At first glance, the fact that the experimental trend is not mirrored by the model results might suggest that the assumption of phase equilibrium leads to completely erroneous results. However, closer examination allows several important conclusions to be drawn in spite of the apparent discrepancy between the model and reality.

The model assumes vapour/liquid equilibrium at all times during compression and the points shown in Figure 17 are those minimum ambient temperatures which produce a flammable mixture at Top Dead Centre. (For this purpose a value of $\phi = 0.61$ as given by Hagen [8] was taken to be the lean flammability limit for methanol/air mixtures in a spark-ignition engine). Only fuel vapour was used to calculate ϕ for this purpose since combustion occurs only in the vapour phase. As a result of the fact that methanol is a single component fuel, adding additional fuel does not change the quantity of vapour present at a given temperature and pressure. Consequently, if equilibrium is maintained, then the only effect of enriching the mixture is to add mass. Since this extra mass absorbs energy from the heating of the air during compression, the effect of extra fuel is to reduce the vapour/air equivalence ratio. The predicted curve for methanol at constant manifold pressure therefore rises as ϕ

increases because the only effect of enrichment is a reduction in temperature when phase equilibrium obtains. The effect of decreasing manifold pressures, as ϕ is increased through choking, is to improve vaporization. This largely counteracts the rise in the predicted curve due to increased fuel mass; hence, the actual manifold pressure curve is essentially flat. Figure 17 shows that phase equilibrium is not maintained which is consistent with the results seen in Figure 16; however, the value of minimum starting temperature predicted is in fact very close to the limiting value actually measured at higher fuel/air ratios. It can thus be concluded that improvement in cold-starting due to choking is caused by the increased evaporation rate provided by the additional surface area of the extra droplets. Thus, as droplet surface area increases, the evaporation rate speeds up, more closely approaches phase equilibrium and hence approaches the theoretical curve. Beyond an equivalence ratio of about seven, both experimental and theoretical curves indeed begin to rise because the extra fuel mass is finally beginning to attenuate the temperature rise.

Considering improved atomisation as a means of improving methanol cold-starting, it is evident that the theoretical curve (using actual manifold pressure) defines the limit of improvement possible through smaller drop size.

Figure 18 shows the predicted and calculated minimum starting temperatures for Indolene (a lean limit of $\phi = 0.75$ [9] was used as the criterion). In this case, the fundamental difference between single component and multicomponent blends is apparent. Unlike the results for methanol seen in Figure 17, increasing equivalence ratio in the mathematical model does improve cold-starting (even at constant manifold pressure) because of the vaporization of the additional light ends present. The effect of the increasing fuel mass as an attenuator of temperature rise again makes itself felt but only much later because the effect of evaporation of light ends predominates in the first part of the curves. The experimental curve is still dropping at the maximum fuel/air ratio possible in this apparatus, but it would also be expected to rise eventually as the extra fuel mass begins to affect the temperature rise during compression. One of the reasons that the experimental methanol curve starts to rise so much sooner than that of Indolene is the fact that there is about twice

as much fuel mass with methanol as with gasoline for a given equivalence ratio. Based on the methanol results of Figure 17, the gasoline curve of Figure 18 could be expected to flatten out at around $\phi = 15$.

Because the lean flammability limits of the gasoline/methanol blends are unknown, a theoretical comparison of cold-starting cannot realistically be compared to experimental data at present. The curve is a similar shape to that of Indolene but is displaced vertically depending on the assumed lean limit. Until relevant data on flammability limits is generated, the comparison must wait.

However, the fuels can be compared on a slightly less direct basis. Figure 19 shows a comparison of the predicted vaporization of the three fuels having the same gasoline base stock. It is interesting that both M10 mixtures evaporate more than Indolene early in the compression stroke but fall behind as the piston approaches Top Dead Centre. Given similar lean limits, it would therefore be expected that both would start less easily than Indolene, for these conditions at least i.e., both would require a higher equivalence ratio. Figures 8 and 9 confirm that both fuels do indeed require higher equivalence ratios at a given temperature.

8/ CONCLUSIONS

1/ Specific cold-starting performance data have been obtained under carefully controlled conditions for pure methanol, the commercially prepared M10 mixture supplied by the Ministry and two M10 blends made up from Indolene base stock.

2/ The OMTC M10 exhibited slightly improved cold-starting behaviour compared to Indolene over most of the temperature range except around -40°C where it performed slightly worse. Both specially prepared M10 mixtures performed worse than Indolene.

3/ The choke is much less effective as a starting aid for pure methanol than for gasoline.

4/ The fundamental volatility characteristics of pure methanol preclude significant improvements in cold-starting performance merely through better atomisation.

5/ Engine combustion system improvements are required before pure methanol can provide cold weather operation acceptable in the Canadian climate.

6/ The mathematical model in its present stage of development can define the limit of cold-starting possible for a single component fuel like methanol. However, for fuel blends, evaporation rate effects predominate; therefore, the present equilibrium-based model is not adequate to predict the cold-starting limit.

7/ The next step required in the mathematical modelling is the incorporation of evaporation rate calculations.

8/ Phase separation remains a problem for gasoline/methanol blends. It would be very useful to conduct tests on the two liquid phases separately, so as to evaluate the effect of complete stratification in an automotive fuel tank.

9/ There is a need for experimental data on the flammability limits of M10 mixtures. In order to be useful for cold-starting calculations, the limits would have to be determined for the components evaporating in about the first 30% of the fuel.

REFERENCES

1/ Methods for the Measurement of Fluid Flow in Pipes," British Standard No. 1042, British Standards Institution, London, 1964.

2/ Standard Handbook for Mechanical Engineers, 8th Edition, T. Baumeister, Editor, McGraw-Hill, New York, 1978.

3/ Annand, W.J.P., "Heat Transfer in the Cylinders of Reciprocating Internal Combustion Engines," Proc Instn Mech Engr, Vol. 177, No. 36, 1963.

4/ Lange's Handbook of Chemistry, 11th Edition, J.A. Dean, Editor, McGraw-Hill, New York, 1973.

5/ Bardon, M.F. and Rao, V.K., "Calculation of Gasoline Volatility," Work in preparation for publication, Department of Mechanical Engineering, Royal Military College of Canada.

6/ Bridgeman, O.C., "Equilibrium Volatility of Motor Fuels from the Standpoint of Their Use in Internal Combustion Engines," Research Paper RP 694, National Bureau of Standards, U.S. Dept of Commerce, 1934.

7/ "Distillation of Gasoline, Naphtha, Kerosene and Similar Petroleum Products," Test D86, American Society for Testing and Materials, Philadelphia, 1978.

8/ Hagen, D.L., "Methanol as a Fuel: A Review with Bibliography," SAE paper No. 770792 for meeting, Detroit, Sept. 26-30, 1977.

9/ Obert, E.F., Internal Combustion Engines and Air Pollution, Intext, New York, 1973.

10/ "Vapour Pressure of Petroleum Products (Reid Method)," Test D323, American Society for Testing and Materials, Philadelphia, 1979.

APPENDIX A

PROPERTIES OF THE FUELS TESTED

1/ ASTM Distillation [7]

Percent Evaporated	Temperature (°C)			
	Indolene (RVP=61.7 kPA)	M10 (RVP=61.7 kPA)	M10 (RVP=80.0 kPA)	OMTC M10 (RVP=68.9 kPA)
IBP	34	45	33	34
5	51	52	44	42
10	63	56	50	47
20	77	67	56	49
30	91	80	62	54
40	101	99	95	66
50	111	110	108	83
60	118	120	118	103
70	128	133	131	125
80	145	145	149	151
90	166	167	179	181
95	183	184	203	214

2/ Specific Gravity:

Indolene -- 0.744
M10 (RVP = 61.7 kPA) -- 0.761
M10 (RVP = 80.0 kPA) -- 0.750
OMTC M10 -- 0.734

3/ Functions f_1 and f_2 in the Vapour Pressure Relation [Equation 13] are functions of vapour fraction VF having the following form:

$$y = C_0 + C_1VF + C_2VF^2 + C_3VF^3 \qquad (15)$$

Molecular weight was also expressed in the form of Equation 15.

4/ Methanol vapour pressure was found using Equation 12 with the following values for the constants:

A = 7.0224
B = 1474.08
C = 44.02
(T in K P_{sat} in kPA)
Molecular weight for methanol was taken to be 32.

5/ Other thermodynamic data used were as follows:

Property	Indolene	M10 (RVP=6.7 kPA)	M10 (RVP=80.0 kPA)	Methanol
C_p vapour (kJ/kg K)	1.65	1.65	1.65	1.38
C_p liquid (kJ/kg K)	2.09	2.09	2.09	2.56
h_{fg} (kJ/kg) (T_o = 298°R)	411-115 VF	360-60 VF	373-70 VF	1169

TABLE A-1 -- Values of Constants in Equation 15

Constant		Fuel		
		Indolene	M10 (RVP=61.7 kPA)	OMTC M10
f_1^*	C_0	0.81934×10^{9}	0.11761×10^{10}	0.14535×10^{10}
	C_1	-0.10443×10^{10}	-0.25692×10^{10}	0.31119×10^{10}
	C_2	0.15363×10^{10}	0.30931×10^{10}	-0.10971×10^{11}
	C_3	-0.94461×10^{9}	-0.13186×10^{10}	0.68039×10^{10}
f_2^*	C_0	0.30706×10^{4}	0.31224×10^{4}	0.31715×10^{4}
	C_1	0.15292×10^{4}	0.73315×10^{3}	0.24599×10^{3}
	C_2	-0.15822×10^{4}	0.57515×10^{2}	0.76308×10^{3}
	C_3	0.80883×10^{3}	-0.12640×10^{3}	-0.33587×10^{3}
MW	C_0	0.69453×10^{2}	0.71299×10^{2}	0.67822×10^{2}
	C_1	0.70384×10^{2}	0.32654×10^{2}	0.84981×10^{1}
	C_2	-0.70678×10^{2}	0.64036×10^{1}	0.36494×10^{2}
	C_3	0.37888×10^{2}	-0.60069×10^{1}	-0.12795×10^{2}

*Values shown give vapour pressure in P_a when T is in K in Equation 13

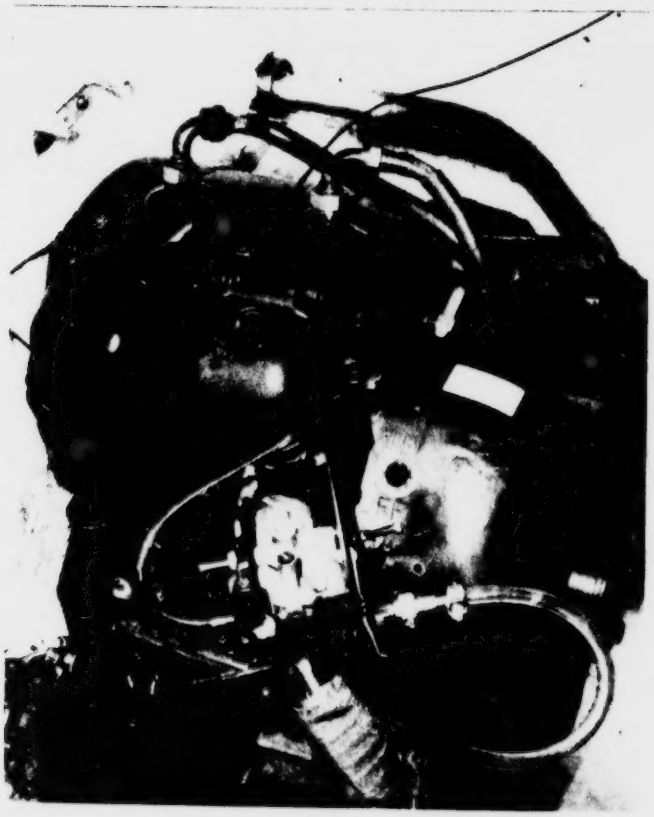

Figure 1/ Test Engine

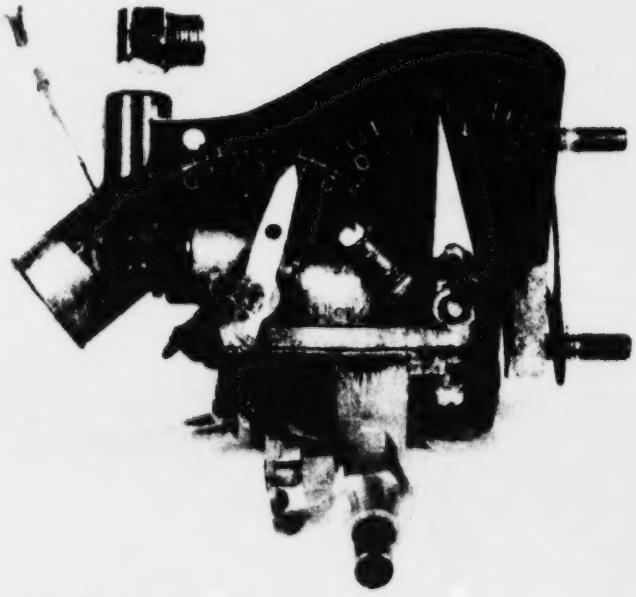

Figure 2/ Carburettor Fitted with Positioning Jigs to Provide Precise Choke and Throttle Openings

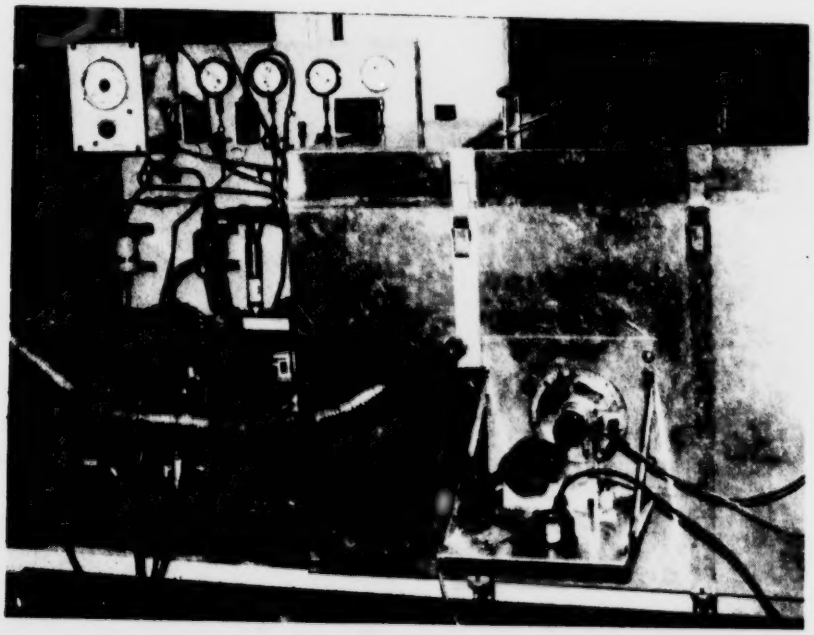

Figure 3/ Cold Chamber Showing Variable Speed Cranking Motor (centre front) and Refrigeration Unit (left)

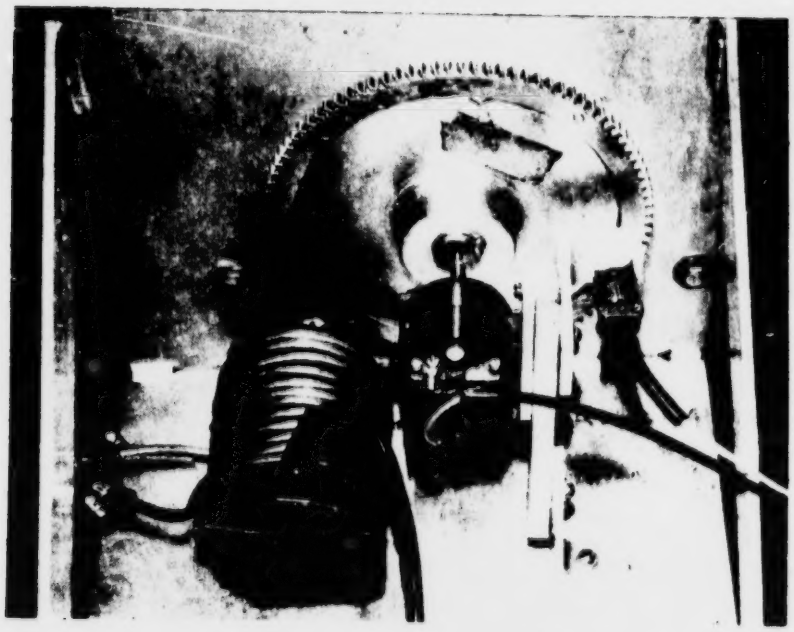

Figure 4/ Cranking Motor Arrangement

The copper tubing coiled around the motor is for cooling. A small electric tachometer is mounted coaxial with the engine crankshaft. The pickup on the right is a transducer to indicate crank angle from Top Dead Centre.

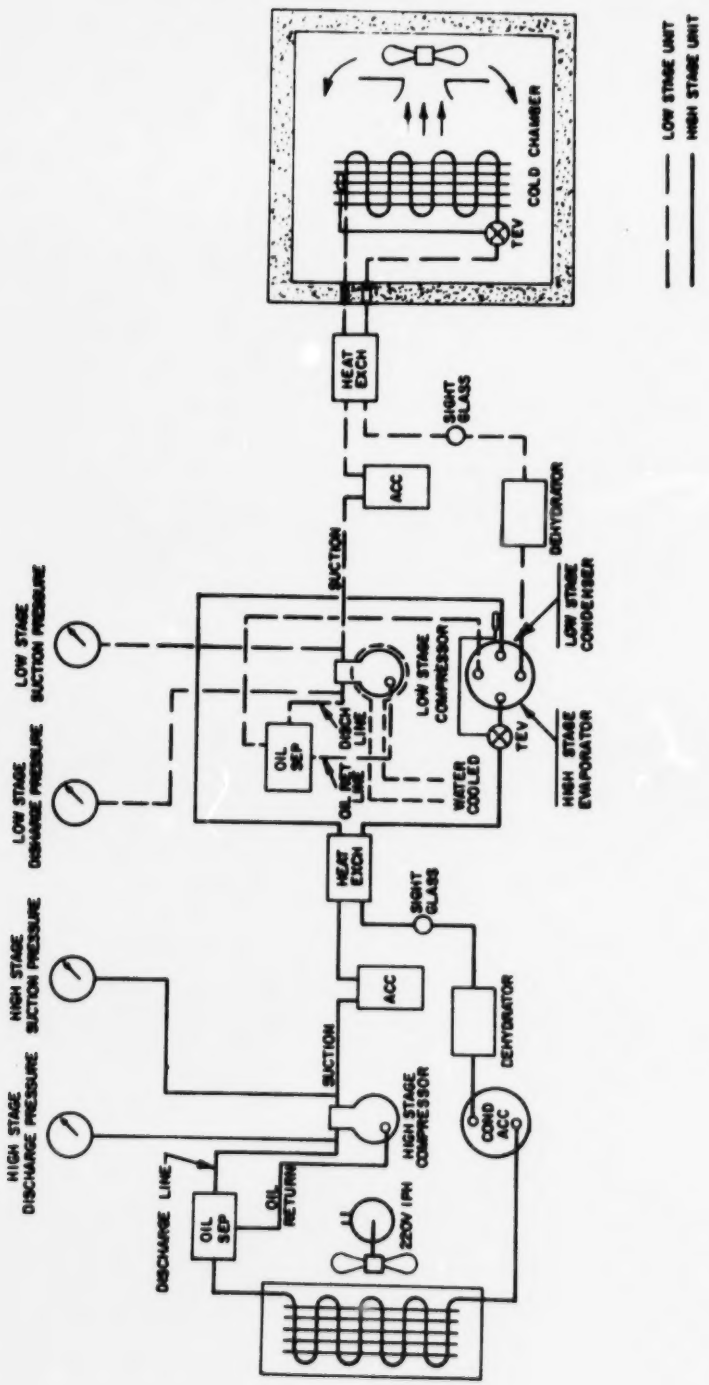

Figure 5/ Schematic of Two-Stage Cascaded Refrigeration Unit and Cold Chamber

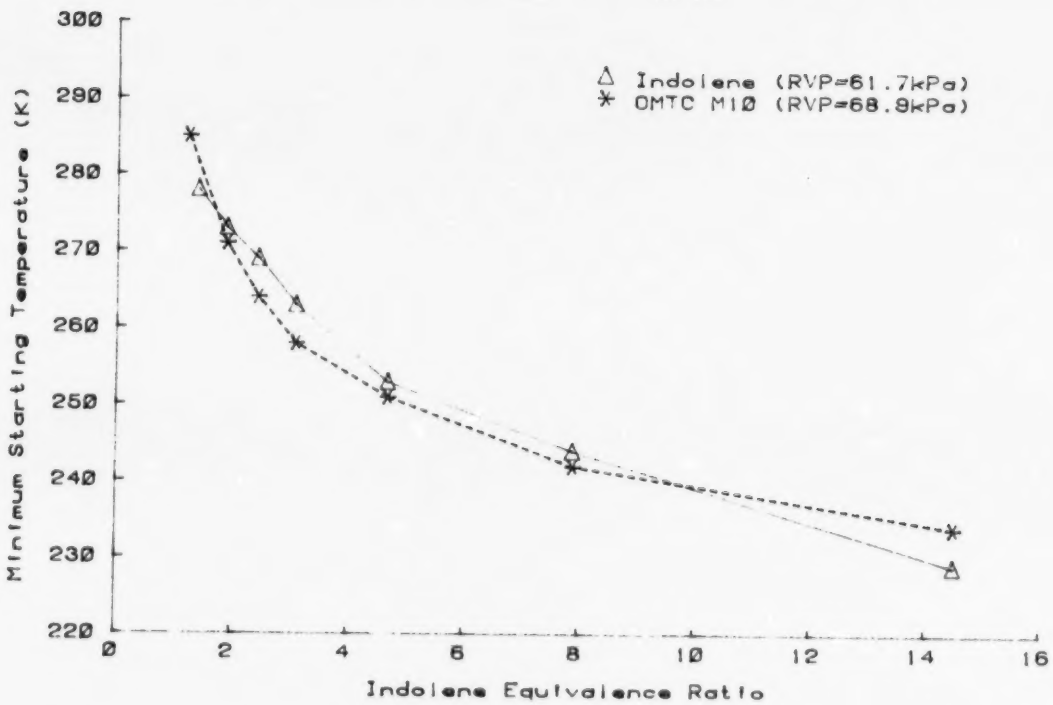

Figure 6/ Comparison of the Cold-Starting Performance of Indolene and OMTC M10 for Identical Carburettor Settings

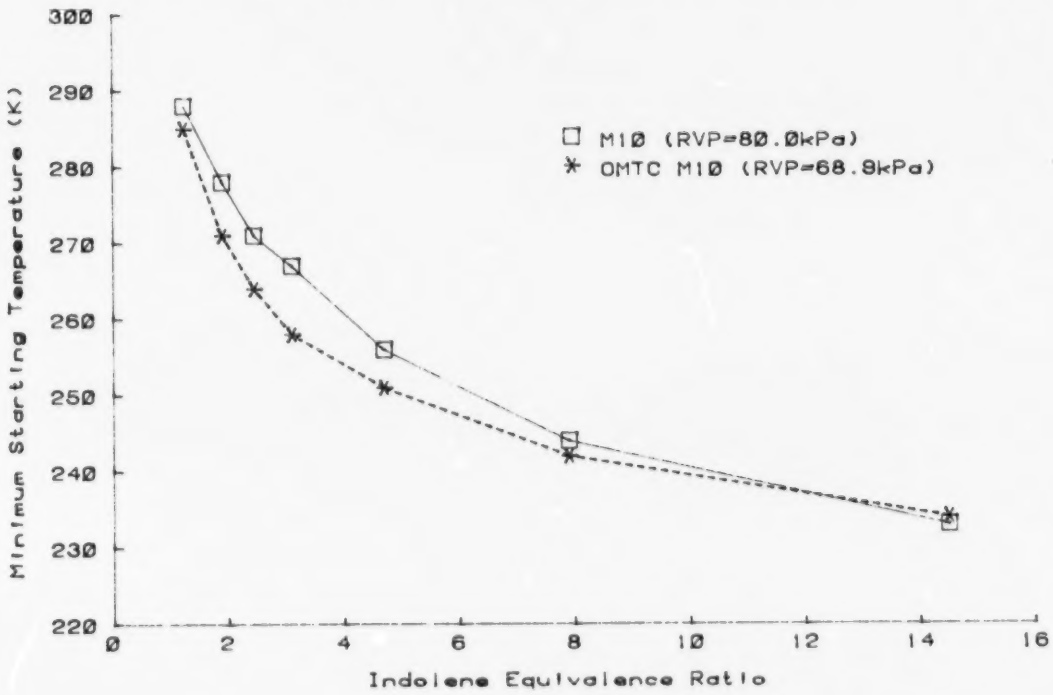

Figure 7/ Comparison of the Cold-Starting Performance of OMTC M10 and High Volatility M10

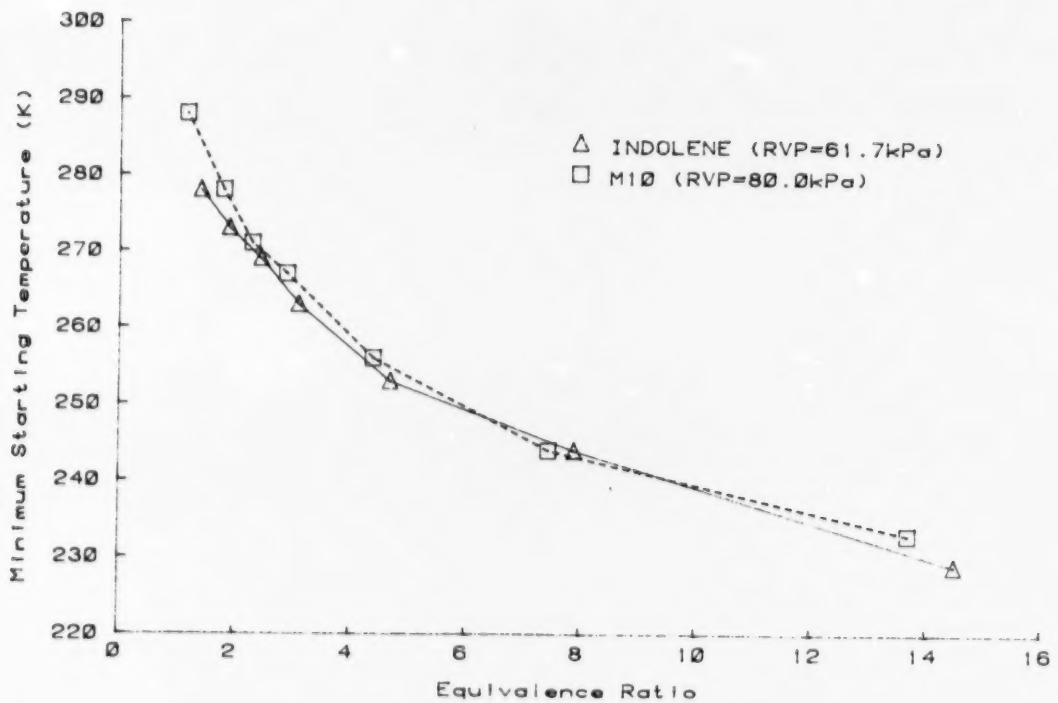

Figure 8/ Comparison of the Cold-Starting Performance of Indolene and High Volatility M10

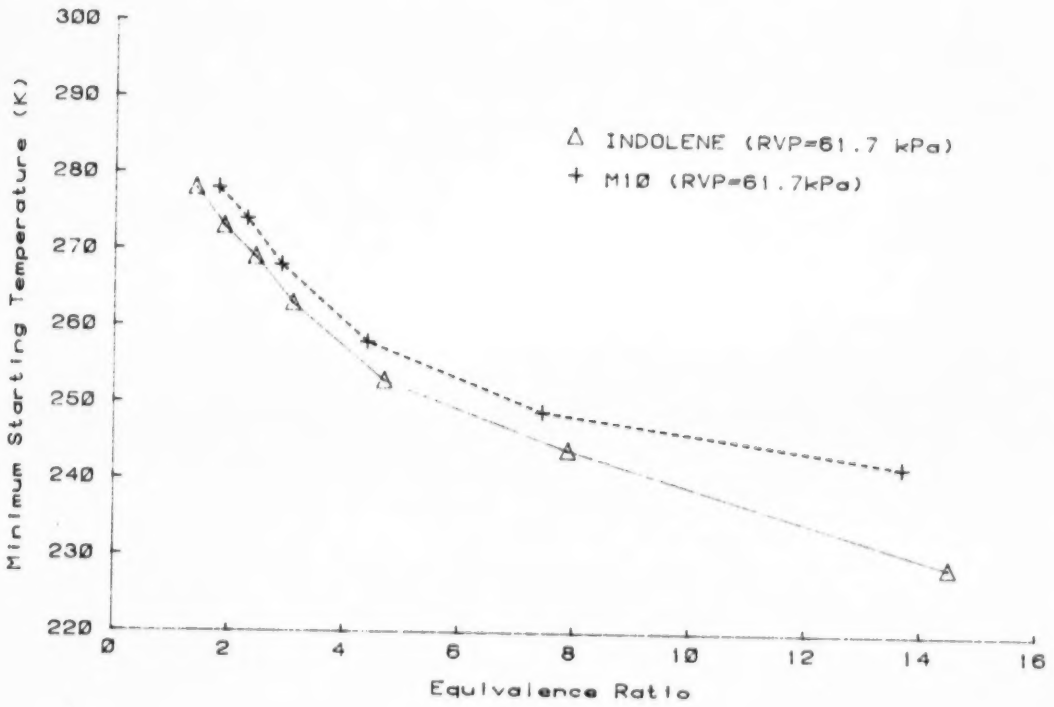

Figure 9/ Comparison of the Cold-Starting Performance of Indolene and M10 of Equal RVP

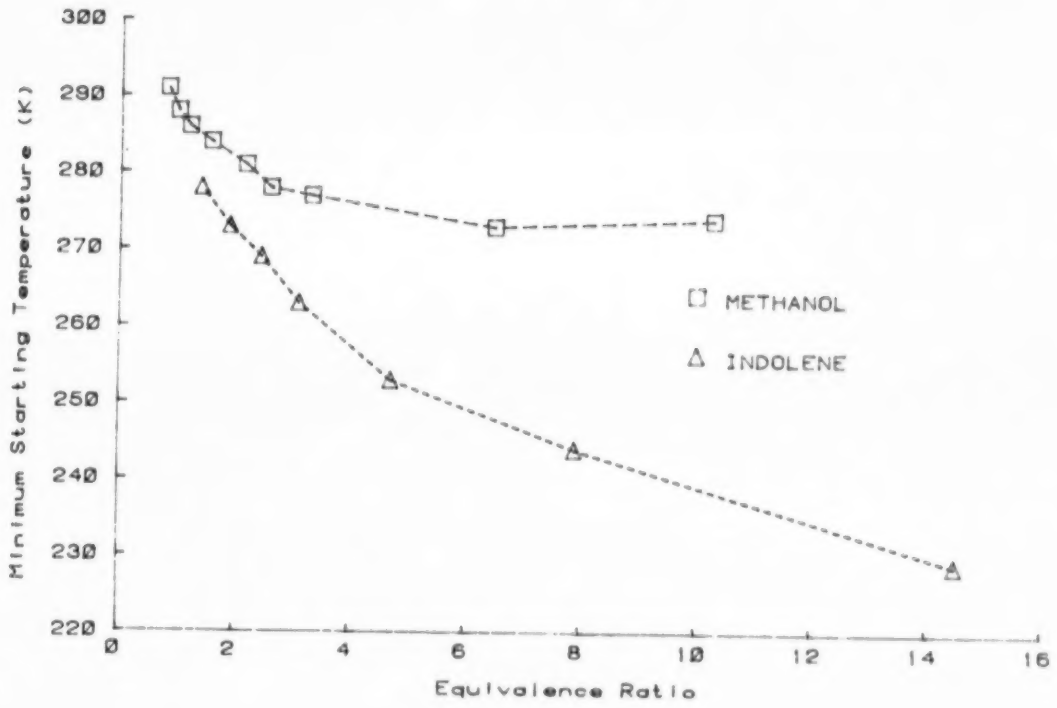

Figure 10/ Comparison of the Cold-Starting Performance of Methanol and Indolene

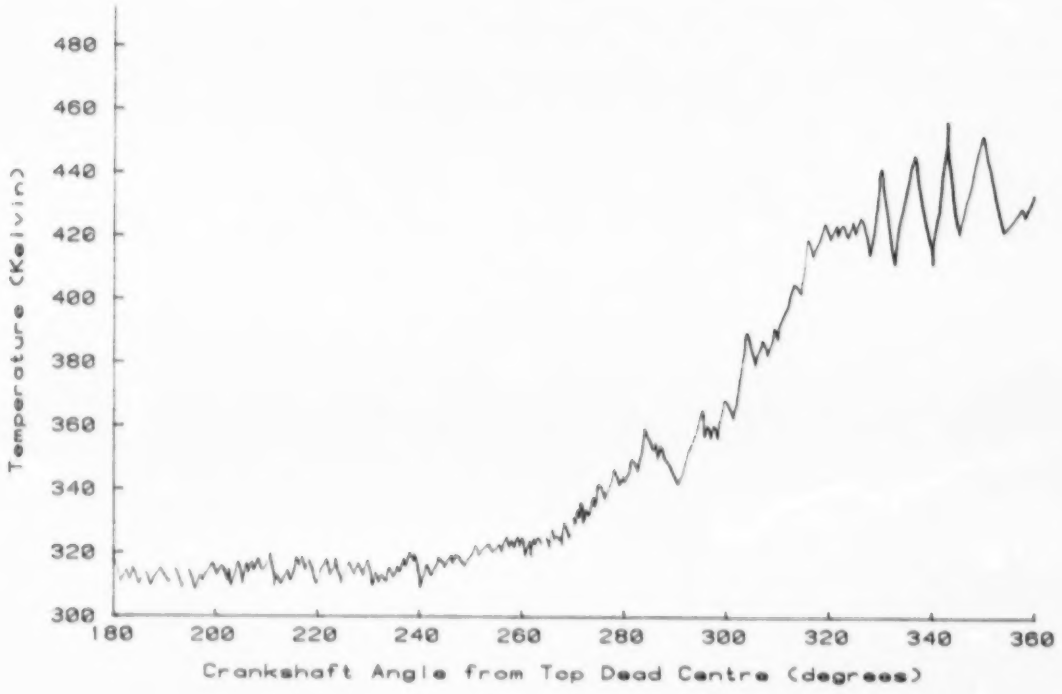

Figure 11/ Measured Cylinder Temperature During the Compression of Air Alone

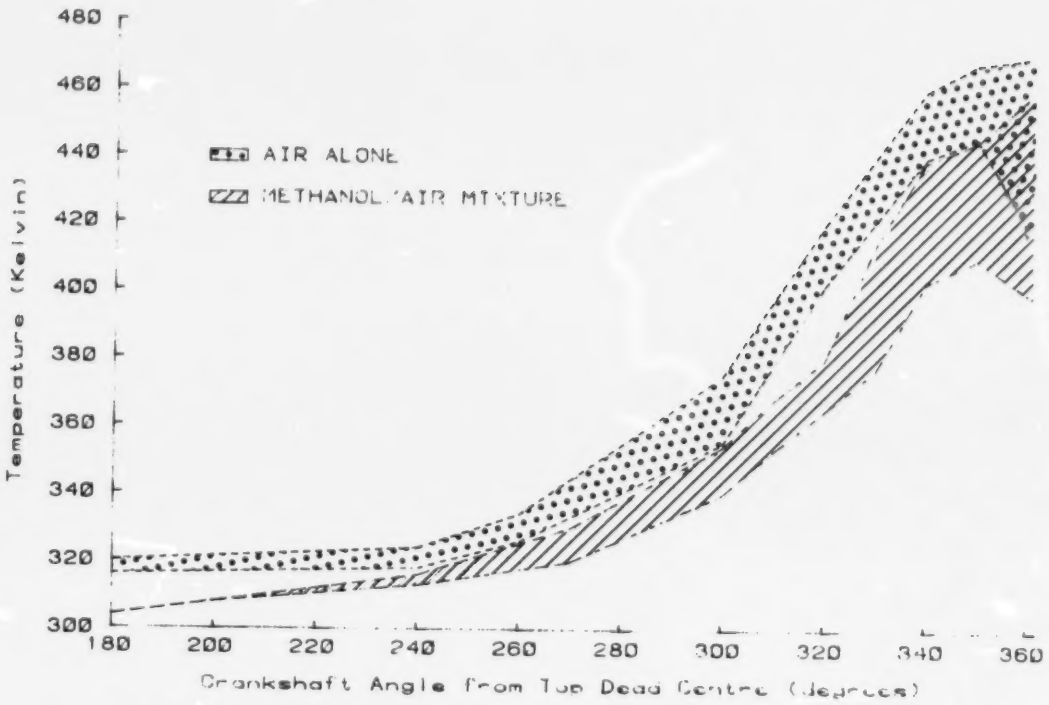

Figure 12/ Measured Cylinder Temperature Bands for Air Alone and Air/Methanol (ϕ = 4)

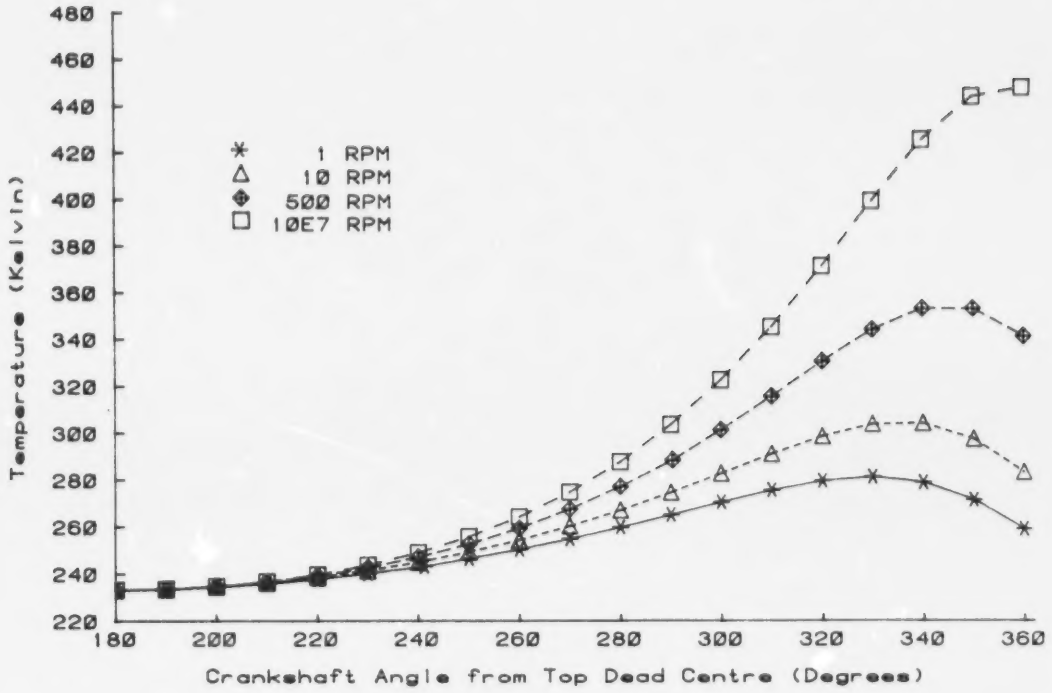

Figure 13/ Effect of Cranking Speed on Temperature Inside the Cylinder (Air Alone)

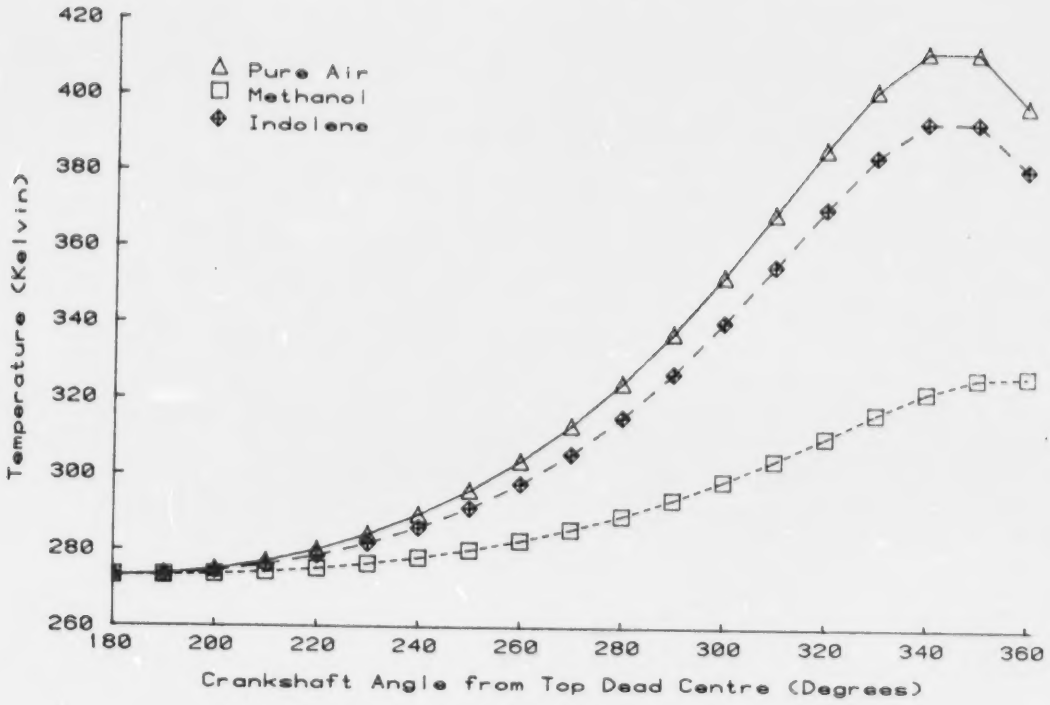

Figure 14/ Predicted Effect of Fuel Evaporation on Temperature Inside the Cylinder

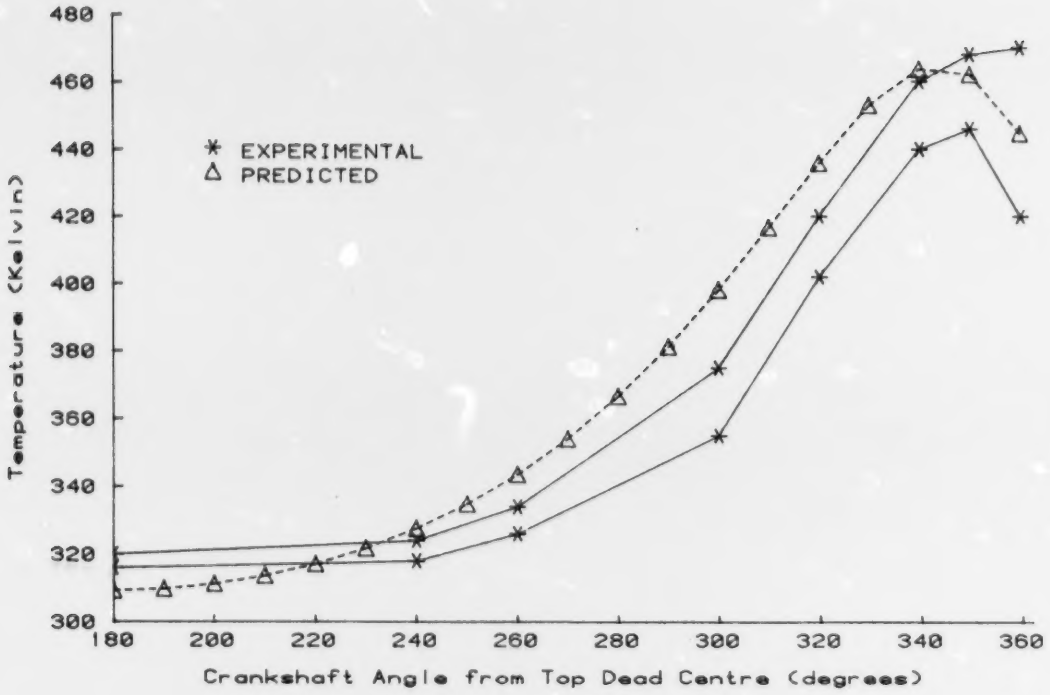

Figure 15/ Comparison of Predicted and Measured Cylinder Temperature (Air Alone)

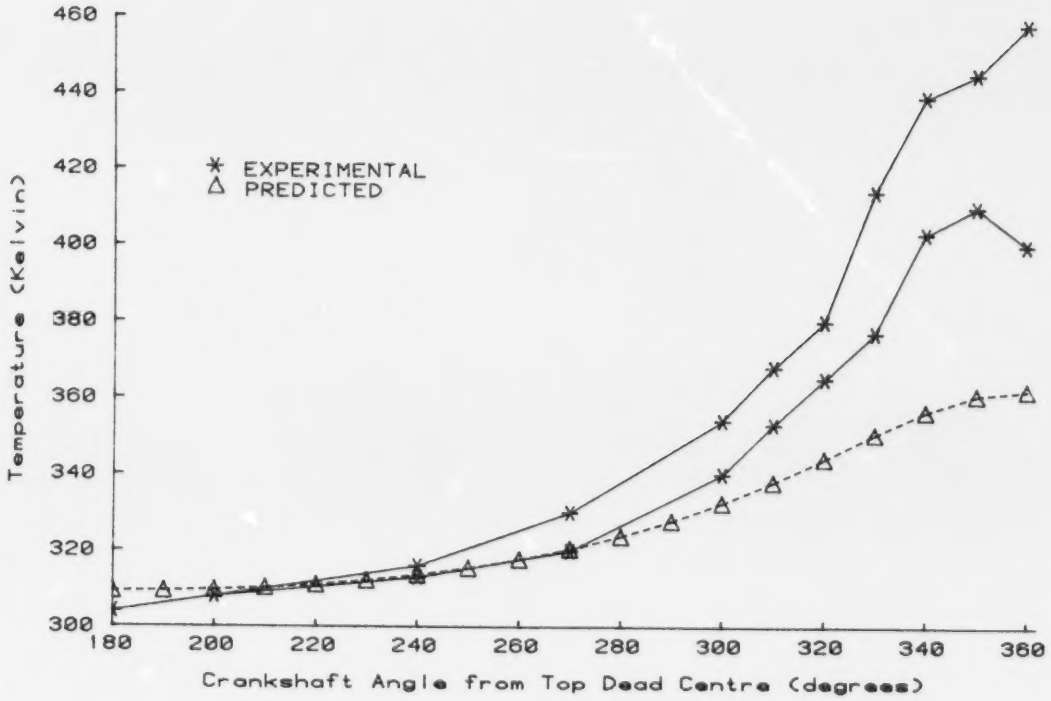

Figure 16/ Comparison of Predicted and Measured Cylinder Temperature Methanol/Air Mixture (ϕ = 4)

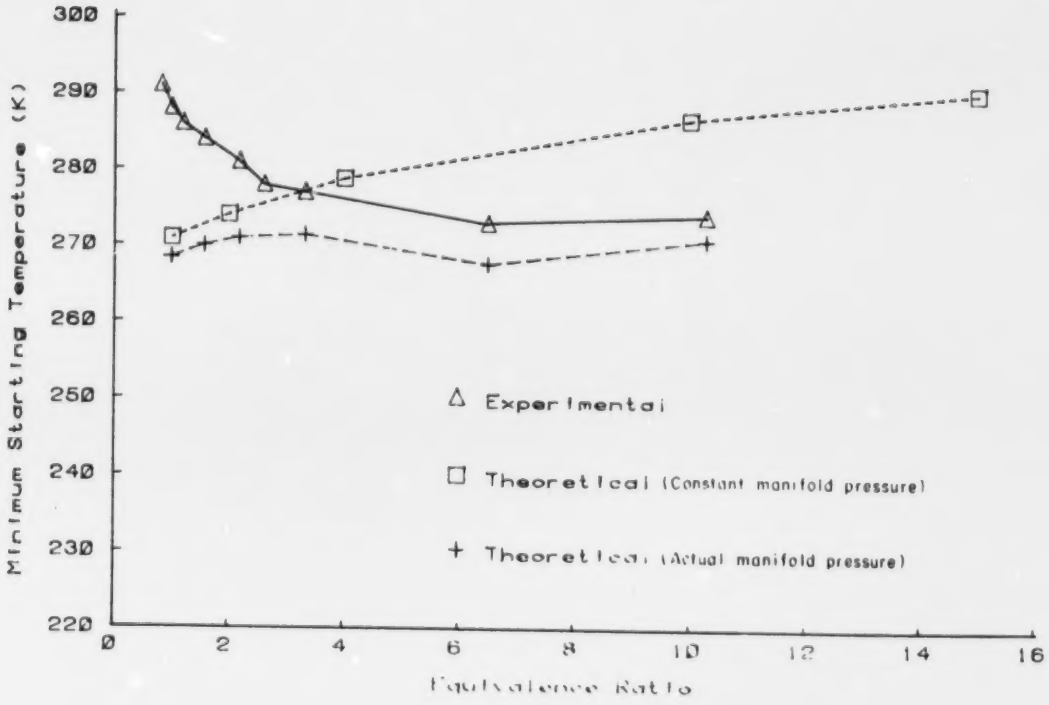

Figure 17/ Predicted and Experimental Minimum Starting Temperature for Methanol

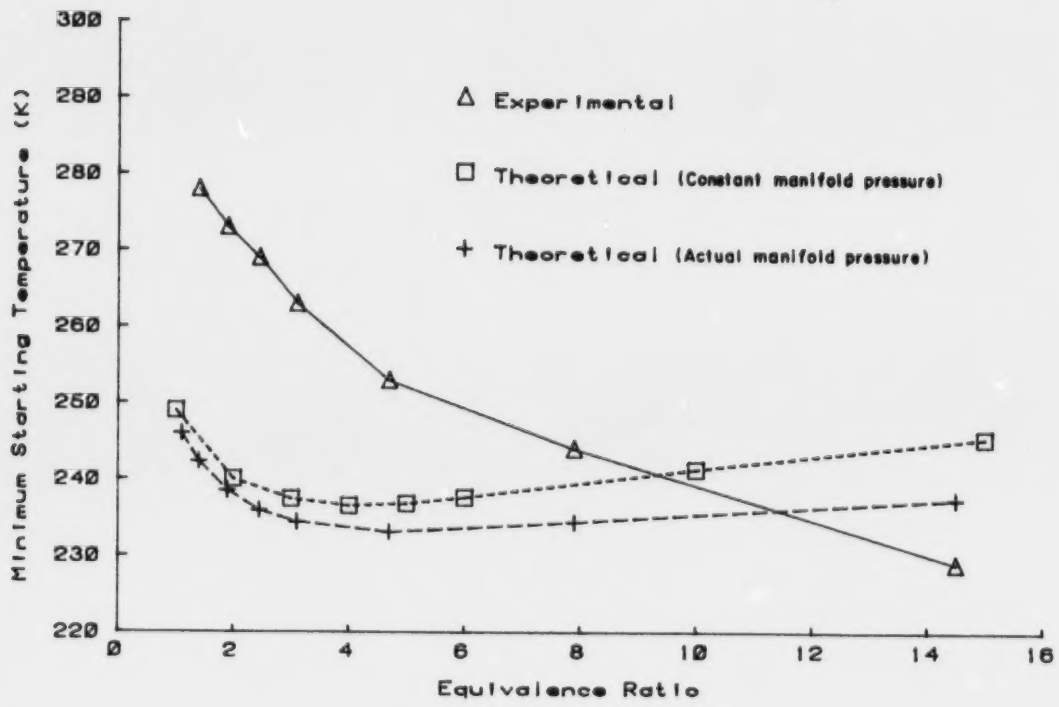

Figure 18/ Predicted and Experimental Minimum Starting Temperatures for Indolene

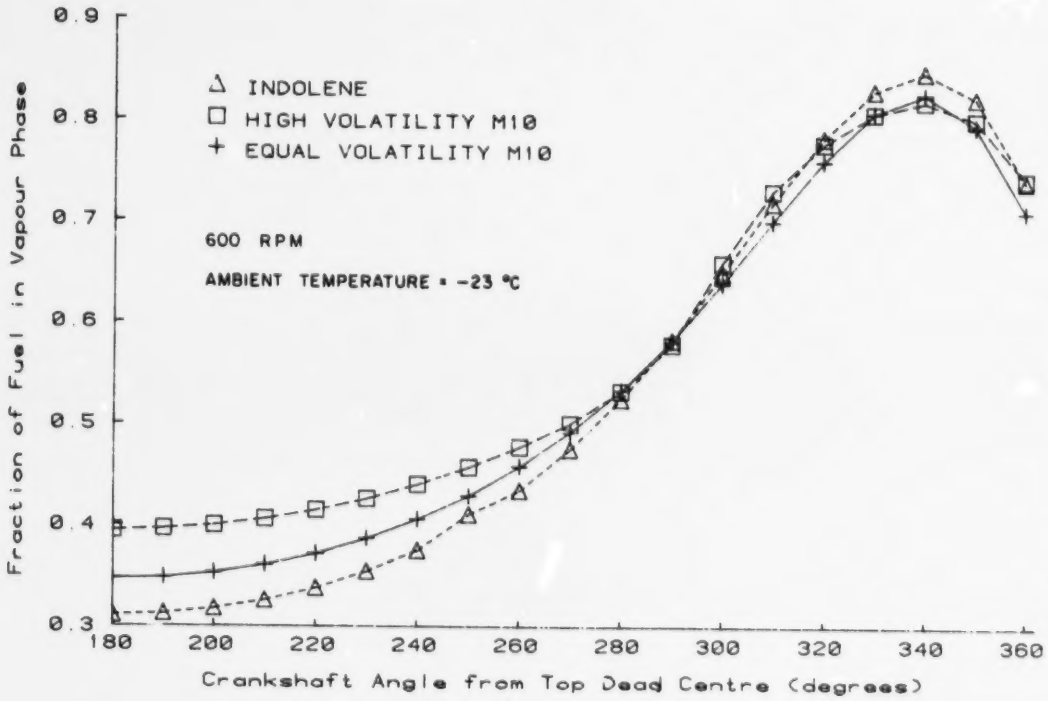

Figure 19/ Predicted Extent of Vaporization of Indolene and Two M10 Mixtures